Proceedings of ASME Turbo Expo 2011
GT2011
June 6-10, 2011, Vancouver, British Columbia, Canada

GT2011-45114

Numerical Investigations on the Leakage Flow Characteristics of Pocket Damper Seals

Zhigang LI, Jun LI*, Zhenping FENG
Institute of Turbomachinery, Xi'an Jiaotong University, Xi'an 710049, China
* Tel/Fax: +86-29-82668704, E-Mail: junli@mail.xjtu.edu.cn

Jiandao YANG, Rui YANG, Liqun SHI
Shanghai Electric Power Generation Technology R&D Center, Shanghai 201108, China

ABSTRACT

The effects of pressure ratios, rotational speeds and sealing clearances on the leakage flow characteristics of pocket damper seals (PDS) were numerically investigated using Reynolds-Averaged Navier-Stokes (RANS) solutions. The leakage flow rate of the experimental PDS with the eight-bladed and eight-pocket was conducted at three different pressure drops and three different rotational speeds. The numerical results were in agreement with the experimental data. Six pressure ratios, four rotational speeds and four sealing clearances were utilized to study the effects of theses factors on the leakage flow characteristics of the PDS. Numerical results show that the leakage rate of the PDS increases with decreased pressure ratio. The leakage rate decreases with the increasing rotational speed, and this phenomenon is more pronounced at higher rotational speed. At the highest rotational speed 20200rpm, the flow coefficient is up to 4.4% less than that of the non-rotating case. The leakage rate increases linearly with sealing clearance increasing. The comparison of the leakage flow rate shows that the PDS leaks slightly less than that of the labyrinth seal at the same pressure ratio, rotational speed and sealing clearance, especially at the higher rotational speed case. Furthermore, the circumferential partition wall can significantly decrease the circumferential flow in the PDS cavity. At the highest rotational speed with 20200rpm, the swirl ratio in the active and inactive cavity of the PDS is reduced by 94.5% and 46% compared to the labyrinth seal, respectively.

NOMENCLATURE

$a=\sqrt{\kappa R_g T_{in}}$	speed of sound[m/s]
A	clearance cross sectional area[m^2]
C_D	discharge coefficient
E	modulus of elasticity for shaft material[N/m^2]
g	acceleration due to gravity[N/kg]
H	dimensionless cavity depth
m	leakage flow rate[kg/s]
$M_{\tan}=U/a$	circumferential Mach number
n	rotational speed[rpm]
P	pressure[Pa]
R	rotor radius[mm]
$R_g=287.2$	specific gas constant[J/kgK]
S	sealing clearance[mm]
$S_r=S/R$	relative sealing clearance
T	temperature[K]
$U=\omega\cdot R$	rotor circumferential velocity[m/s]
U_{gas}	fluid circumferential velocity[m/s]
κ	ratio of specific heats
$K=\left\|U_{gas}/U\right\|$	swirl ratio
ω	angular velocity[rad/s]
ϕ	flow coefficient
ψ	pressure coefficient
$\pi=P_{stat,out}/P_{tot,in}$	pressure ratio
ζ	relative leakage flow rate
β	slop conversion factor
Δ	difference
δ	weight per unit volume of shaft material[N/m^3]
υ	Poisson's ratio for shaft material

Subscripts

$1,2,\ldots i,\ldots,8$	the i-th cavity
ax	axial direction
in/out	inlet / outlet condition
$stat/tot$	static / total value
PDS/LAB	pocket damper seal / labyrinth seal

INTRODUCTION

Rotating fluid seals are critical components serving a significant purpose to enhance the aerodynamic performance of modern turbomachinery, where the leakage flows between stationary and rotating components are one of the main sources for losses[1]. Traditionally, dynamic seals are widely used in compressors and turbines for the control of the leakage flow through rotor-stator clearances from high pressure regions to low pressure regions. Rotating seals are recognized as a major source of destabilizing forces inducing flow excitation and resulting in rotordynamic instability problems since the 1960s, and the first published describing the rotordynamic instability due to the leakage flows in rotating seals was proposed by Thomas[2]. Recently, turbomachinery are being designed to run at higher temperatures, higher pressures and higher speeds. This has resulted in a challenging task in turbine industries to research and develop higher performance dynamic sealing technique which has an optimum balance between leakage characteristics and rotordynamic performance[3,4].

Labyrinth seal, a non-contact dynamic sealing technology, are commonly applied in turbomachinery because the labyrinth seal has excellent benefits of long life-time, easy maintenance, simple design and high temperature capability[5]. The sealing effect of labyrinth seals is achieved by a succession of contractions and expansions. The fluid pressure energy is converted into kinetic energy at each narrow gap between the rotating and static parts. Then, the kinetic energy is either dissipated into heat by turbulence, or enters the subsequent tooth gap by kinetic energy carryover. Therefore, the effectiveness of dissipation of kinetic energy through a series of cavities between throttles determines the leakage flow rate of labyrinth seals. Labyrinth seals are good in effectively limiting the leakage across regions of unequal pressure but do not respond well to rotordynamic and often lead to turbine instabilities[5]. Recently developed dynamic damper seals have been essential to reduce the leakage flow rate and to increase rotordynamic stability of turbomachinery. The dynamic damper seals such as honeycomb seals[7], hole-pattern seals[8], and pocket damper seals(PDS)[9] are employed to avoid the problem of turbine instability and have successfully eliminated subsynchronous vibrations in several high pressure compressors and turbines.

Vance [9] firstly proposed the PDS (Fig. 1) at Texas A&M University. Vance measured leakage and direct damping coefficients of a two-bladed four-pocket PDS and a conventional labyrinth seal. Test results showed that the PDS has fifteen times more direct damping than that of the conventional labyrinth seal. He also showed how the new design is different from the conventional labyrinth seals and honeycomb seals. Different from the labyrinth seal, the PDS is made up of a series of blades dividing the seal into active and inactive cavities and a series of circumferential partition walls separating active cavities into pockets. The PDS is normally designed with active cavities of longer pitch length and with notches on the exit blades of the active cavities. Empirical results and theoretical analysis on the PDS illustrated that these partition walls greatly reduce circumferential flow and these notches result in desired overall positive direct damping by causing an effective diverging clearance in active cavities. The PDS has high direct damping and no destabilizing cross-coupled stiffness and can significantly decrease rotor vibration amplitudes. Therefore, the PDS can be used to replace the conventional labyrinth seals at the effective locations for rotor damping in turbines.

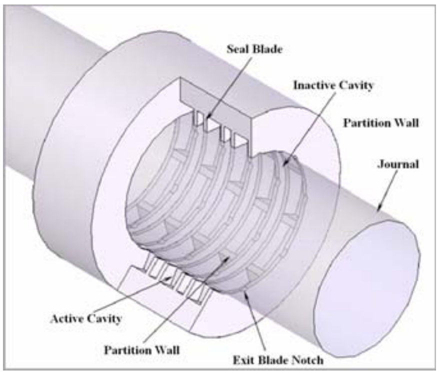

Fig. 1 Ten-bladed PDS[15]

The rotordynamic characteristics of the PDS are associated with the reliability of turbomachinery and therefore worthy of study. Extensive experiments and numerical studies have been conducted in the past[10-13]. However, the leakage reduction remains an important purpose of the PDS. In addition, the stiffness and damping of the PDS are highly dependent on the leakage flow rate and the pressures in the cavities of the PDS. Therefore, investigations on the leakage flow characteristics of the PDS are crucial for the efficient, safe and steady operation of turbomachinery.

Recently, researches[6,15,19] on the leakage flow characteristics of the PDS were mainly based on experimental tests and analytical predictions. Advanced experimental techniques together with numerical methods based on a bulk-flow model have been applied to obtain the leakage characteristics of the PDS. In addition, several relevant parameters influencing the flow characteristics have been identified.

The tests of a six-bladed labyrinth seal and two types of four-bladed PDS with four pockets and eight pockets were conducted by Laos[12]. He observed that the leakage flow rate of the PDS is less than that of the labyrinth seal even if the labyrinth seal has more blades. This result was explained by the reduction of the circumferential flow in the PDS due to the partition walls. Laos[14] also measured the damping and leakage rate of a two-bladed hybrid brush PDS (BHS) of which the downstream blades are replaced by a brush seal element. The results indicated that the brush hybrid PDS has lower leakage rate than that of the six bladed labyrinth seal, although the BHS has only one cavity and the labyrinth seal has five cavities.

Numerical predictions and experimental measurements on the leakage rate and the cavity pressure of the PDS operating at high pressures were conducted by Gamal et al. [15]. Two types of PDS with twelve-bladed and eight-bladed were experiment measured. The leakage rate and cavity pressure measurements were conducted on straight-through and diverging-clearance configurations for each type seal. The blades of the eight-bladed PDS have a rectangular profile, whereas the twelve-bladed PDS have a double-beveled profile. In addition, the inlet blades of each active cavity are beveled on the upstream side and the exit blades are beveled on the downstream side of the PDS. Measurement results showed that the leakage rate of the twelve-bladed PDS was higher than that of the eight-bladed PDS at the same pressure drop and rotational speed. Gamal suggested that the differences in blade profile and cavity pitch length were the main contributing factors to this result.

The experimental research on the PDS conducted by Childs and Vance[16] indicated that the blade profile can significantly affect leakage rates. Ertas[17] studied the influence of blade profile on the leakage characteristics of the PDS. Ertas tested a six-bladed PDS with rectangular-profiled blades at first, then this seal was retested with bevels machined into the downstream sides of the blades. The results showed that the leakage rate of the PDS with beveled blades was 15%~20% higher than that of the seal with rectangular-profiled blades. This result supports the conclusions obtained by Gamal[15].

Vance[18] tested the leakage rate and rotordynamic coefficients of the PDS in the non-rotating and rotating tests. In his experiments, a two-bladed four-pocket PDS and a conventional labyrinth seal were tested at identical conditions. The comparison of the results showed that the leakage rate of the PDS is 30% higher than that of the conventional labyrinth seal. The leakage increases linearly with the increasing inlet pressure for both seals, but the leakage rate of the PDS increases more quickly than that of the conventional labyrinth seal.

A one-control volume, turbulent bulk-flow model for the prediction of the seal leakage and rotordynamic force coefficients of the PDS was presented by Li et al. [19]. Comparisons to measurement results from a two-bladed four-pocket showed that the one-control volume, turbulent bulk-flow model predicts the mass flow rate reasonably accounting for about 20% measurement uncertainty. The leakage rate obtained from this model increases with the increasing inlet pressure, but showed an unusual drop at the choke pressure with 0.325MPa. Li et al [20-22] experimentally investigated the rotordynamic force coefficients and leakage rate of a four-bladed, four-pocket PDS and a two-bladed four-pocket PDS. Li et al presented a comparison of experimental results to analytical predictions based on the one control-volume bulk-flow model [19]. The predicted flow rate increasing linearly with the pressure ratio agreed well with the measurements. Both tests and analytical predictions showed that rotor speed has a negligible influence on the mass flow rate of the PDS when the rotational speed is less than 6000rpm.

The internal fluid dynamics mechanics theory of the PDS is more complex than that of the conventional labyrinth seals due to the complex three-dimensional geometrical topologies. The rotordynamic coefficients of the PDS and leakage rates of seals are highly dependent on the fluid fields in the seals' pockets and pressures in seals' cavities. Nevertheless, no detailed information is available for the flow field in the PDS. In addition, the influence of sealing clearance and rotational speed on the leakage performance of the PDS is seldom presented.

In order to obtain a more detail insight into the flow mechanisms which are responsible for the rotordynamic and leakage characteristics of the PDS, three-dimensional Reynolds-Averaged Navier-Stokes(RANS) solution is applied in this work. The main objective of this work is to utilize a 3D RANS solver approach to investigate the leakage characteristics of a eight-bladed eight-pocket PDS (Fig. 2) and point out the flow phenomena of this seal. At first, the leakage flow rates of the PDS were computed and compared to the experimental data[15]. The numerical results were in agreement with the experimental data. The accuracy and reliability of the utilized numerical method was demonstrated. The influences of pressure ratios, sealing clearances, and rotation speeds on the leakage flow characteristics of the PDS were investigated in detail. For comparison, numerical investigations on the leakage characteristics were also carried out on the conventional labyrinth seal.

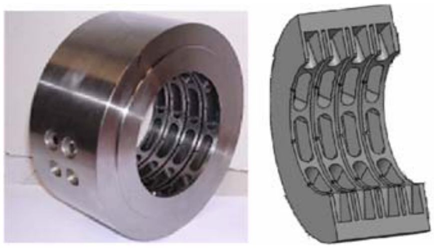

Fig. 2 Eight-bladed PDS[15]

NUMERICAL APPROACH

Computational Model

Fig. 3 shows two different configurations of the eight-bladed PDS[17]: (1) 1:1 clearance ratio(no notches) and (2) 1:1.5 clearance ratio(with notches). The clearance ratio represents the ratio of the inlet blade annular clearance area of active cavities to the exit blade annular clearance area of active cavities. For the 1:1 case, the inlet and exit areas are equivalent, and this configuration is labeled as a "straight through" seal with no notches. For the 1:1.5 case, the exit blades were notched with rectangular notches which serve to make the exit clearance area equal to one and half times of the inlet clearance area, and the configuration is referred to as a diverging seal with notches.

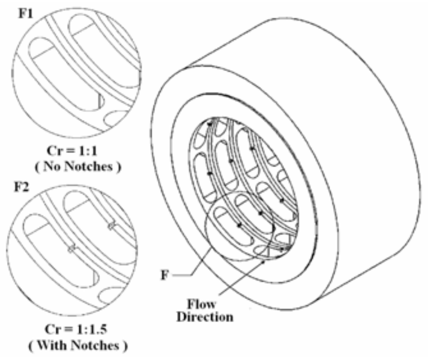

Fig. 3 Geometries of the eight-bladed PDS with and without notches[17]

The experimental "straight through" PDS with no notches was utilized as the computational model in this study. A cross-sectional view of the "straight through" PDS is shown in Fig. 4. This seal consists of four circumferential rows of eight equally spaced active cavities, which are axially separated by three annular inactive cavities. The computational geometrical parameters of the experimental research are obtained from

Gamal [15] and listed in Table 1. For the comparison of leakage characteristics between the PDS and the conventional labyrinth seal, the investigations have also been carried out for a conventional labyrinth seal.

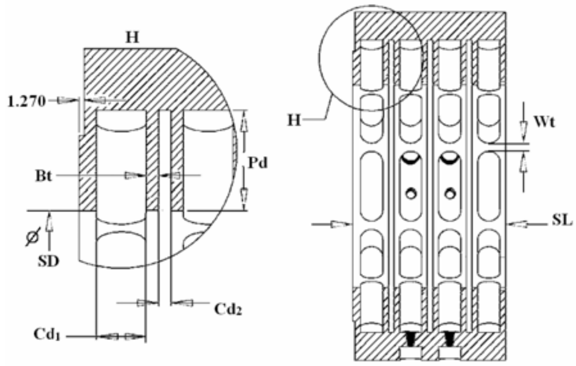

Fig. 4 Geometrical parameters of eight-bladed PDS without notches[17]

Table 1 Major dimensions of test seals[15]

Geometrical parameter	Nomenclature	Value
Seal length	SL/mm	87
Inner diameter	SD/mm	114.55
Radial inlet clearance	*S*/mm	0.13
Clearance ratio	Cr/-	1:1
Number of blades	Num1	8
Pocket depth	Pd/mm	25.4
Number of pockets	Num2	8
Partition wall thickness	W_t/mm	5.08
Blade thickness	B_t/mm	3.18
Active cavity length	Cd_1/mm	12.7
Inactive cavity length	Cd_2/mm	3.18

Numerical Method

The flow in the PDS is quite complex turbulent flow due to the 3D geometry and flow conditions. Therefore, it is necessary to solve 3D RANS equations to analyze the flow patterns, and to predict the leakage flow characteristics of the seals.

Multi-block structured grid was generated for the PDS and the conventional labyrinth seal using grid generation software ANSYS ICEM. Fig. 5 shows the computational grids and corresponding boundary condition definitions for the PDS and conventional labyrinth seal. The 3D geometry and boundary condition definitions of the PDS are shown in Fig. 5(a). Fig. 5(b) gives the local calculated mesh for the PDS. Numerical investigations were carried out for the PDS with four clearance sizes $S1 = 0.13mm$, $S2 = 0.18mm$, $S3 = 0.22mm$, and $S4 = 0.25mm$. The computational grids and boundary condition definitions of the conventional labyrinth seal are shown in Fig. 5(c). For the conventional labyrinth seal, the numerical investigations have been focused on the smallest clearance size $S1 = 0.13mm$. Geometrical parameters of the PDS and the conventional labyrinth seal are the same except for the partition wall. In order to simulate the flow in two computational seals at minimal computational cost, the axial symmetric properties of the seal geometry were considered. The periodic boundary condition was assumed in the circumferential direction. One pocket with 1/8 circumference segment of the PDS and 1/120 circumference segment of the conventional labyrinth seal was modeled, respectively.

The commercial finite volume CFD software ANSYS CFX 11.0 [23] was used to simulate the leakage flow characteristics of the PDS. This software solves the compressible RANS equations. A second order high resolution discretization scheme was used. The turbulence characteristics of the flow were modeled by the standard $k-\varepsilon$ equations. The scalable logarithmic wall function [23] was used to describe the near wall velocity. According to the CFX user guide, the scalable logarithmic wall function was utilized when the $y^+/4$ is greater than 11.06, therefore the grid near wall was carefully monitored to ensure the proper range of y^+. The overall y^+ range is 40-200 for the geometry regions of two computational seals. The y^+ criterion is met over almost the entire wall region.

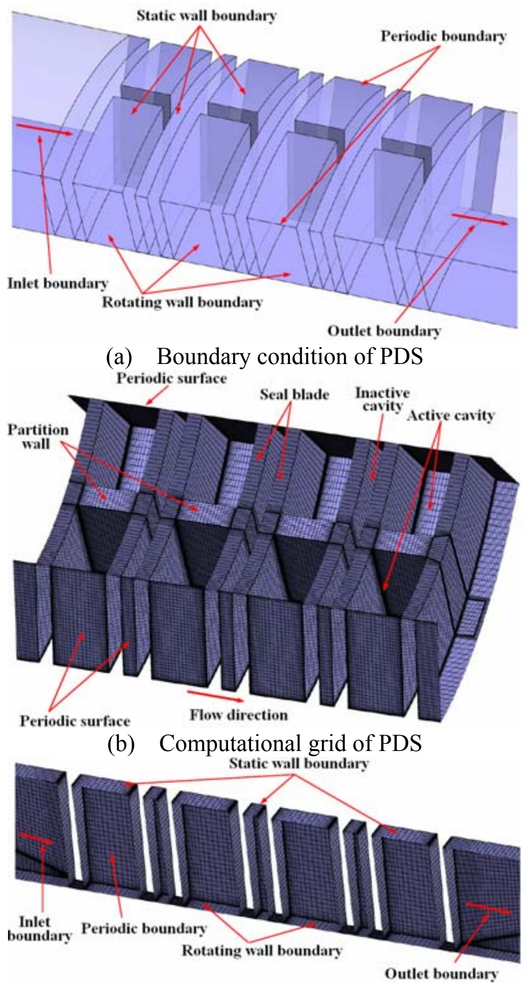

(a) Boundary condition of PDS

(b) Computational grid of PDS

(c) Conventional labyrinth seal

Fig. 5 Computational mesh and boundary condition definition

Table 2 Conditions and numerical methods

Inlet total pressure	6970 - 7212 kPa
Inlet total temperature	300 K
Outlet static pressure	868 – 3716 kPa
Discretization scheme	High resolution
Computational method	Time marching method
Turbulence model	$k-\varepsilon$, scalable log wall function
Fluid	Air (ideal gas)
Wall properties	Adiabatic, smooth surface

The detailed numerical approaches in the current study are listed in Table 2. As shown in Fig. 5, the inlet boundary was placed at the inlet of the seal, and total pressure, total temperature and turbulence quantities were defined. The averaged static pressure was specified at the outlet of the seal. In addition, the static and rotating walls were defined to be adiabatic. Three rotational speeds with $n1 = 10200rpm$, $n2 = 15200rpm$ and $n2 = 20200rpm$ were specified to the rotating wall boundary. The desired convergent target of each simulation was that the root mean square (RMS) residuals [23] of the momentum and mass equations, energy equation, and turbulence equations reach (or even lower than) 10^{-6}.

To quantify the leakage flow characteristics of the PDS, a semi-empirical leakage analytical model was presented. Assuming that the fluid flow passing through the seal is a perfect gas and is reasonably modeled using isothermal flow with constant values for the pressure and density at each cavity of the seal, the leakage flow rate is described by a semi empirical leakage equation (1) at the unchocked flow condition [24]. The leakage flow rate becomes independent of the downstream pressure and is defined by equation (2) at the chocked flow condition [15].

$$m = C_D \frac{P_{tot,in} \cdot A}{\sqrt{R_g \cdot T_{tot,in}}} \sqrt{\frac{2k}{k-1}\left[(\pi)^{2/k} - (\pi)^{(k+1)/k}\right]} \quad (1)$$

$$m = C_D \cdot \left(P_{tot,in} \cdot A\right) \Big/ \sqrt{R_g \cdot T_{tot,in}} \quad (2)$$

where A represents the area of the annular section formed by the seal blade and the journal, $P_{tot,in}$ is the total pressure at the seal inlet, and $T_{tot,in}$ is the inlet total temperature. The pressure ratio π represents the ratio of the seal outlet static pressure to the seal inlet total pressure.

Based on this analytical model, the leakage flow rates are made dimensionless through the flow coefficient ϕ defined by equation (3) [6]. The cavity pressures are made dimensionless through the pressure coefficient ψ defined by equation (4) [6].

$$\phi = m \cdot \sqrt{R_g \cdot T_{tot,in}} \Big/ \left(A \cdot P_{tot,in}\right) \quad (3)$$

$$\psi = \left(P_i - P_{stat,out}\right) / \left(P_{tot,in} - P_{stat,out}\right) \quad (4)$$

The flow coefficient ϕ is uniquely defined by the pressure ratio, rotational speed, sealing clearance, and characterized by a function of three dimensionless numbers given in (5).

$$\phi = f\left(\pi, M_{\tan}, S_r\right) \quad (5)$$

where $M_{\tan}$ [24] is the dimensionless form of the rotational speed and defined as the ratio of the circumferential velocity of the rotor to the seal inlet sound speed. S_r is the dimensionless form of the sealing clearance and defined as the ratio of the sealing clearance to the rotor radius.

Grid Independence Analysis

The flow coefficient of the experimental pocket damper seal was derived with 382,000, 553,000, 716,000 and 887,000 nodes separately to calibrate the grid independence of the numerical approach. The inlet pressure was kept at 6,984kPa, the pressure drop was 4,626kPa, and the rotational speed was 10,200rpm. The differences between the CFD value and experimental data [15] are about 2.5%, 0.7%, 0.4% and 0.4% respectively, as shown in Table 3. In order to balance the calculation accuracy and simulation time, a 716,000 node mesh is employed in the present numerical study for the PDS.

Table 3 Flow coefficient of the PDS

Grid Number	CFD	EXP[15]
382,000	0.266	
553,000	0.275	0.273
716,000	0.274	
887,000	0.274	

Numerical Method Validation

In order to demonstrate the accuracy and reliability of the numerical approach for predicting the leakage characteristics of the PDS, the effects of rotational speeds and pressure drops on the leakage flow rates of the experimental PDS were calculated and compared with the experimental data. The geometrical parameters and experimental leakage flow rates are adopted from Ref [15]. Fig. 6 gives the comparison of the leakage flow rate of the PDS between the numerical results and the experimental data.

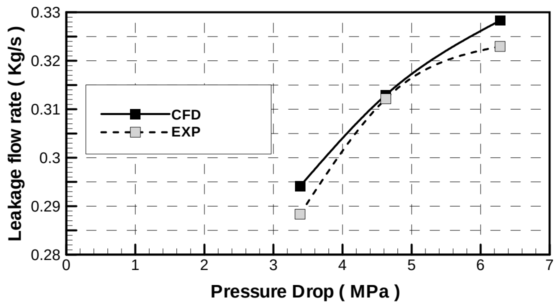

(a) $n1 = 10200rpm$

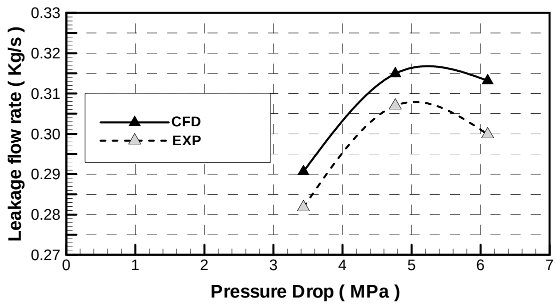

(b) $n2 = 15200rpm$

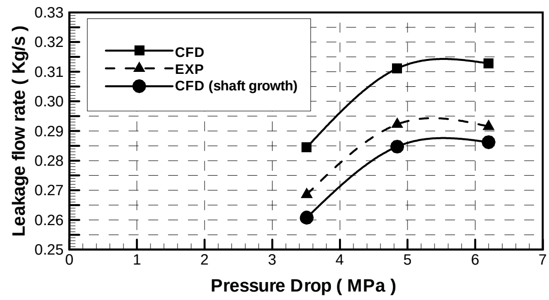

(c) $n3 = 20200rpm$

Fig. 6 Comparison of the leakage flow rate between the present CFD results and the experimental data($S1 = 0.13mm$)

Compared to the experiment data, numerical results over predict the leakage flow rate for all numerical conditions. As shown in Fig. 6, leakage flow rates obtained from the present numerical method and the experimental data agree very well and the maximum relative deviation ($\left(m_{CFD} - m_{EXP}\right)/m_{EXP}$) is 2.0% at the rotational speed $n1 = 15200rpm$. With increasing *n*, the numerical results deviate gradually from the experimental data and the maximum relative deviation is 4.4% and 7.2% at rotational speed $n2 = 15200rpm$ and $n3 = 20200rpm$, respectively. The averaged relative deviation for all numerical cases approximates to 3.8%. This can be explained by the shaft growth at high rotational speeds. Empirical results as well as theoretical analysis have shown that the centrifugal forces acting on the material of the rotor increase and cause the rotor to expand at high rotational speeds. The seal clearance of the PDS studied in present paper is so small that even a small radial expansion of the rotor is significant. The increase in rotor radius is given by equation (6). According to the Ref [15], the inlet blade radial clearances of the test seal are reduced by ~5% at the highest rotational speed $n3 = 20200rpm$. The importance of taking shaft growth into consideration in the PDS applications is made apparent by the effects of sealing clearance on the leakage flow rate in the results and discussions of this paper.

$$\Delta R = \delta\omega^2 / 4gE \cdot (3 + \upsilon) \cdot R_s^3 \tag{6}$$

Fig. 6(c) shows the leakage rate using CFD with consideration of shaft growth effect. Compared to the experiment data, the “CFD (shaft growth)” solutions under predict the leakage flow rate for all the pressure drops with a maximum relative deviation 2.9%. The reliability and accuracy of the utilized numerical approach can be demonstrated.

RESULTS AND DISCUSSIONS

On the basis of the accuracy and reliability of the utilized numerical approach, investigations on the influences of pressure ratios, rotational speeds and sealing clearances on the leakage performance of the PDS were carried out to provide further understanding of the fluid mechanics theory in the PDS. In addition, the calculations of the leakage flow rate were also carried out for the conventional labyrinth seal, and comparisons of the leakage characteristics between the PDS and labyrinth seal were presented.

Effects of Pressure Ratio

To investigate the effect of pressure ratios on the leakage performance of the PDS, six pressure ratios were calculated at three rotational speeds and four clearances. Fig. 7 gives the dependence of the flow coefficient upon the pressure ratio of the PDS. The similar variation behavior of flow coefficients of the PDS with pressure ratios at different rotational speeds and clearances is observed in Fig. 7. The effect of the pressure ratio on the flow coefficient is significant at high pressure ratio. At lower pressure ratio, the flow coefficient begins to show a trend independent of the pressure. For the pressure ratio down to $\pi = 0.26$, the flow coefficient increases with the decreasing pressure ratio, and the change is slowed down gradually. With π decreasing, the flow coefficient asymptotically approaches a maximum value. This can be explained by the fact that when the pressure ratio is low enough to result in the choked flow across the last blade tip gap, and the leakage flow rate will become independent of the pressure ratio.

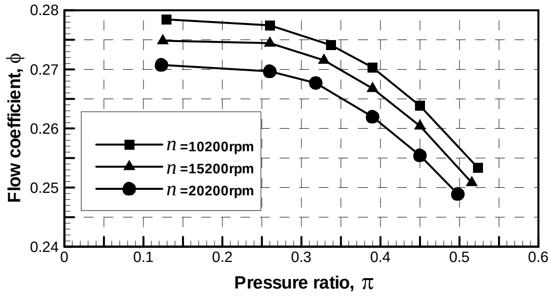

(a) $S1 = 0.13mm$

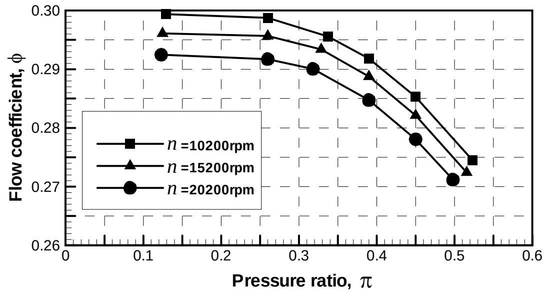

(b) $S2 = 0.18mm$

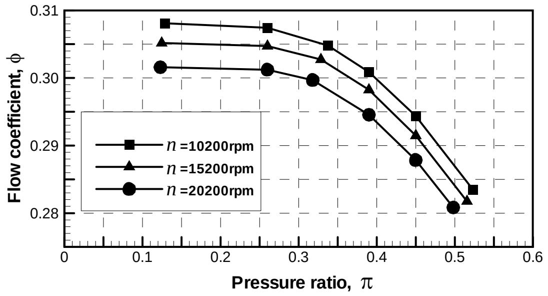

(c) $S3 = 0.22mm$

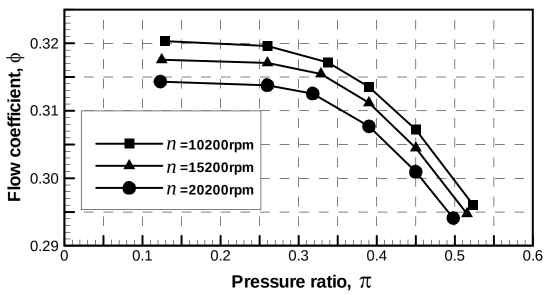

(d) $S4 = 0.25mm$

Fig. 7 ϕ versus π in the PDS at different rotational speeds and sealing clearances

Fig. 8 shows the axial Mach number distribution in the tip gap of the last seal blade at different pressure ratios. The axial Mach number increases with decreased pressure ratio, and the maximum number is presented at the exit of tip gap. The axial Mach number is close to the critical value $M_a = 1.0$ at the pressure ratio $\pi = 0.26$. With π decreasing, the axial Mach number is beyond the critical value, and the chocked flow occurs in the last blade tip gap.

The variation of the maximum Mach number in the last blade tip gap at three rotational speeds is shown in Fig. 9. The influence of the rotational speed on the Mach number does not appear at all pressure ratios. The Mach number reaches to the critical value *Ma*=1.0 at pressure ratio $\pi = 0.22$. This indicates that the chocked flow condition depends on the running pressure ratio for the PDS.

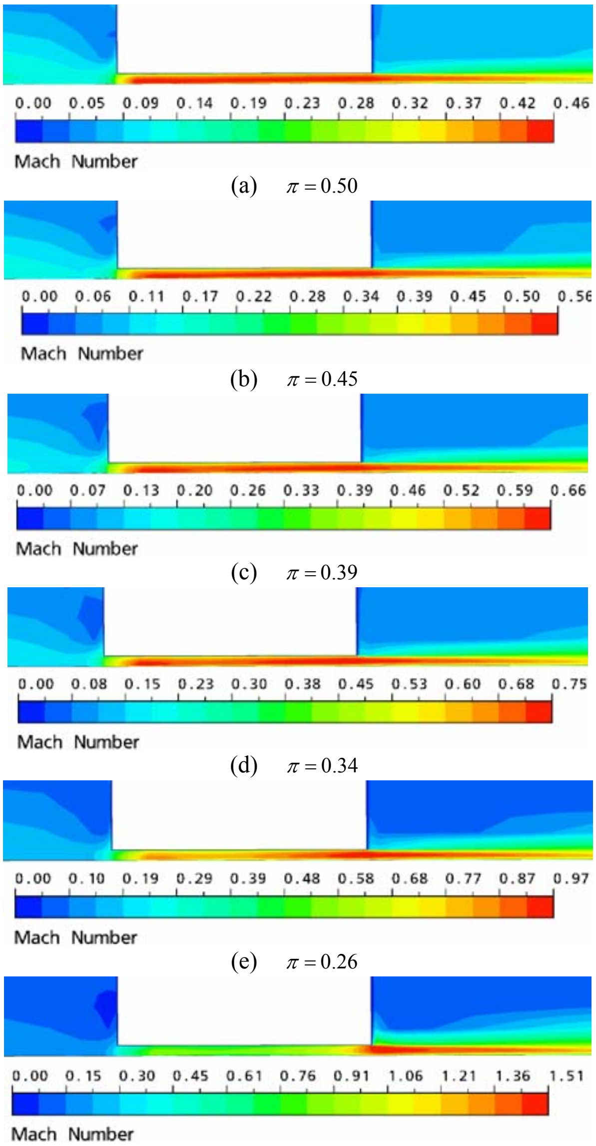

Fig. 8 Axial Mach number distribution in the tip gap of the last seal blade at different pressure ratios ($s1 = 0.13mm$, $n2 = 15200rpm$)

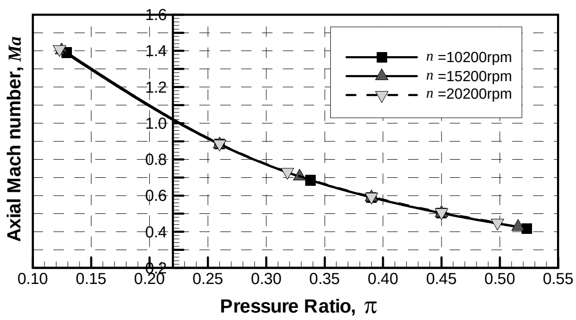

Fig. 9 Axial Mach number in the exit of the last seal blade tip gap at different pressure ratios ($S1 = 0.13mm$)

Effects of Rotational Speed

Numerical simulations were carried out at four rotational speeds including the non-rotating condition to investigate the effect of rotational speeds on the leakage characteristics of the PDS. In Fig. 10, the calculated leakage flow rates of the PDS were plotted as the corresponding dimensionless number ϕ versus the circumferential Mach number $M_{\tan}$, which indicates the rotational speed and takes the seal rotor radius into account. Comparing the curves in Fig. 10 shows that the variation behavior of the flow coefficient with circumferential Mach number at different pressure ratios and sealing clearances are similar. At the fixed pressure ratio and sealing clearance, the flow coefficient decreases with increasing circumferential Mach number, and this trend is more significant at higher circumferential Mach number. At circumferential Mach number $M_{\tan} = 0.35$, the flow coefficient is less than that of the non-rotating case up to 4.4%. It is important to note that these leakage flow rates in Fig. 10 were calculated without taking shaft growth into consideration.

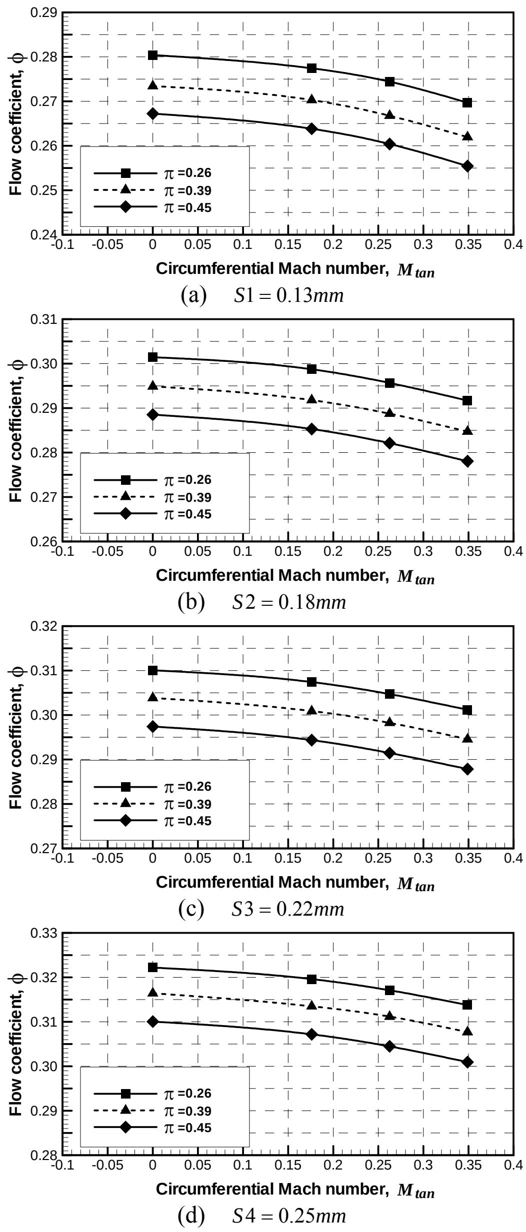

Fig. 10 ϕ versus $M_{\tan}$ in the PDS at different pressure ratios and sealing clearances

Effects of Sealing Clearance

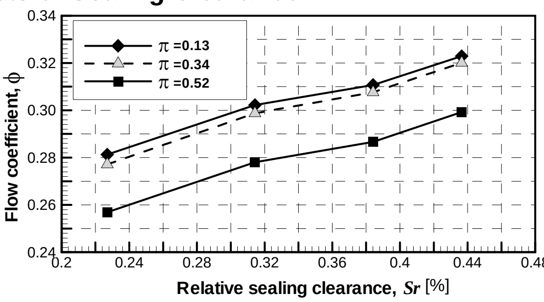

(a) $n = 0rpm$

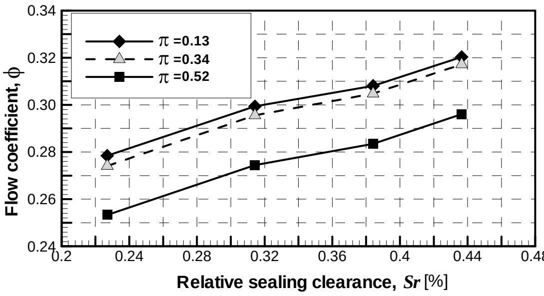

(b) $n1 = 10200rpm$

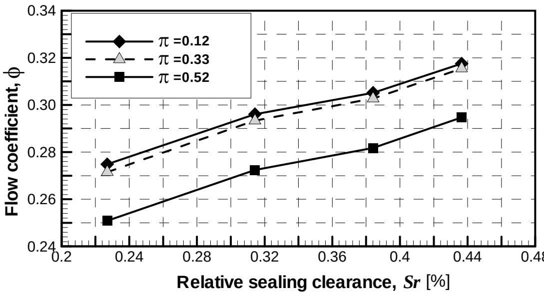

(c) $n2 = 15200rpm$

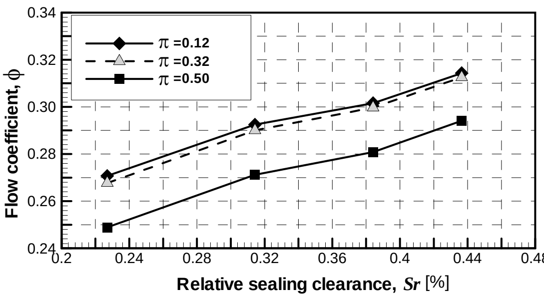

(d) $n3 = 20200rpm$

Fig. 11 ϕ versus S_r in the PDS at different pressure ratios and rotational speeds

Four sizes of sealing clearance between the seal blade tip and the rotor were calculated to investigate the effect of sealing clearances on the leakage characteristics of the PDS. The dependence of the flow coefficient on the relative sealing clearance at different pressure ratios and rotational speeds is illustrated in Fig. 11. The increase in flow coefficient is an approximate linearly proportional to the relative sealing clearance at all pressure ratios and rotational speeds. The similar variation behavior of the curves in Fig. 11 means that the relative sealing clearance has the same effect on the flow coefficient at all pressure ratios and rotational speeds. According to data in Fig. 11, the increase in the flow coefficient with approximate linear characteristics can be obtained from the increase in relative sealing clearance by multiplying a slope conversion factor β defined in Eq. (7)

$$\Delta\phi = \beta \cdot \Delta S_r \quad (7)$$

where $\beta \approx 20.5$. It should be noted that the increased flow area A due to the increasing clearance is already accounted for the flow coefficient ϕ as shown in equation (3).

Effects of Shaft Growth

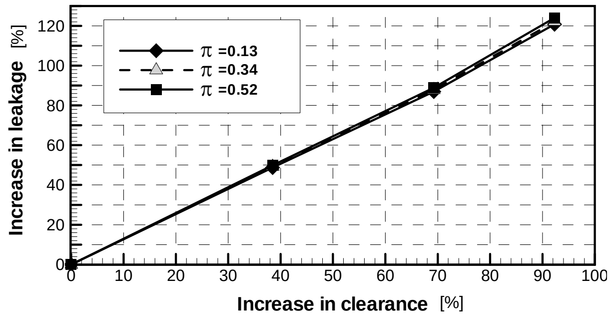

(a) $n = 0rpm$

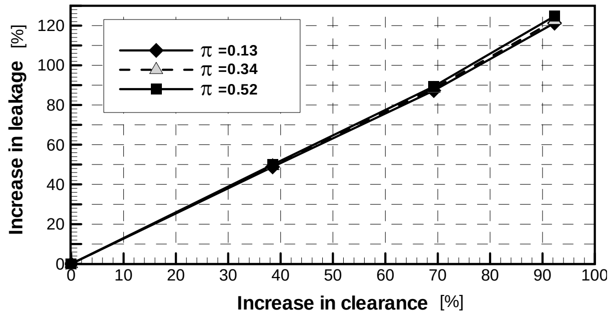

(b) $n1 = 10200rpm$

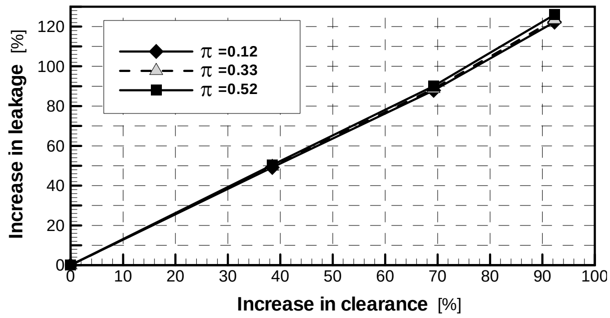

(c) $n2 = 15200rpm$

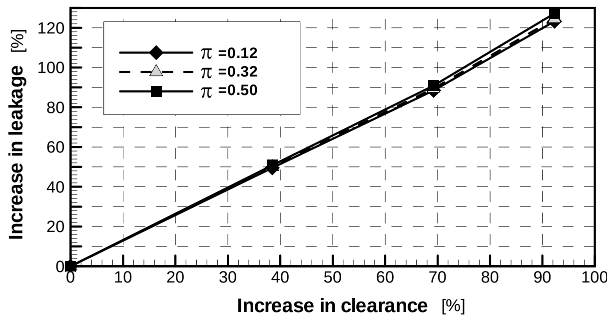

(d) $n3 = 20200rpm$

Fig. 12 Percent increase in leakage versus percent increase in clearance at different pressure ratios and rotational speeds

To demonstrate the significant influence of shaft growth on the leakage performance of the PDS, the relation between the percent increase in leakage flow rate and the percent increase in sealing clearance is given in Fig. 12. Comparison of the curves in Fig. 12, a similar variation in the trend of the increase in leakage among the increase in clearance is observed at different pressure ratios and rotational speeds. The percent increase in leakage linearly increases with increasing percent increase in clearance with slope 1.27. As to the "straight through" PDS investigated in present paper, Ref. [15] pointed out that the inlet blade radial clearances of the seal are reduced by about 5% at the highest rotor speed 20200rpm due to the shaft growth. Based on the data in Fig. 12, it can be expected that the leakage flow rates of the PDS decrease by 6.35% at the highest rotor speed 20200rpm due to the shaft growth. This indicates that it is important to take shaft growth into consideration in the PDS leakage prediction. In addition, this does go some way with explaining the phenomenon that the numerical approach used in present paper over predicts the leakage rate by a larger amount as the rotational speed increases.

Comparison of Leakage Flow Rate and Flow Fields

The influence of the partition wall on the leakage characteristics of the PDS is described by the relative leakage ζ defined in equation (8).

$$\zeta = m_{PDS} / m_{LAB} \quad (8)$$

where m_{PDS} and m_{LAB} represents the leakage flow rate of the PDS and the conventional labyrinth seal, respectively. Except for the partition wall, all other geometrical factors of the conventional labyrinth seal are same with those of the PDS presented in Table 1. m_{PDS} and m_{LAB} were calculated at the same pressure ratio and rotational speed.

The calculated leakage flow rate of the PDS and labyrinth seal is plotted as the relative leakage ζ versus the pressure ratio π at different rotational speeds as shown in Fig. 13. All the values of the relative leakage in Fig. 13 are slightly less than 1.0. In addition, the relative leakage decreases with increasing rotational speed and remains about the same at different pressure ratios. Compared to the labyrinth seal, the PDS reduced the leakage by 0.4% - 1.9% over the range of calculated pressure ratios and rotational speeds. This indicates that the PDS leaks slightly less than the labyrinth seal, especially at the higher rotational speed. This can be explained by the reduction in the circumferential flow in the PDS due to the partition walls as described in Ref. [12].

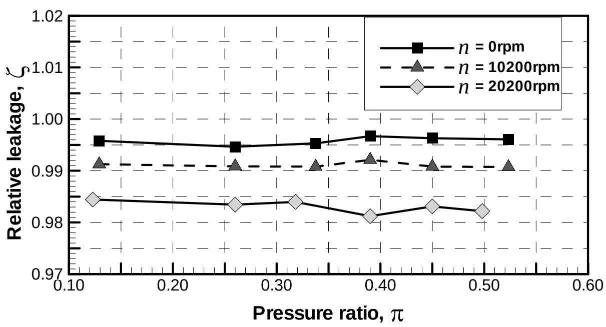

Fig. 13 ζ versus π at different rotational speeds ($s1 = 0.13mm$)

To obtain a more detailed insight into the flow mechanisms that are responsible for the leakage characteristics, the flow fields in the PDS were analyzed and compared to those in the conventional labyrinth seal in the present study. Two dimensionless variables were defined to describe the swirl development in seals. The dimensionless swirl ratio K is defined in equation (9), as the ratio of the fluid circumferential velocity to the rotor circumferential velocity. The dimensionless chamber depth is defined in the equation (10).

$$K = \left| U_{gas} / U \right| \quad (9)$$

$$H = (r - R)/Pd \quad (10)$$

The static pressure and velocity results from numerical simulations in present paper are displayed in several sections at different positions to show the three-dimensional development of the flow field in the PDS. Fig. 14 gives the positions of the six sections. Section 1 represents the meridional surface and Section 2 represents the 50% chamber height surface. Section 3-6 represents the axial section surfaces in the active cavities(C.1,C.3,C.5,C.7).

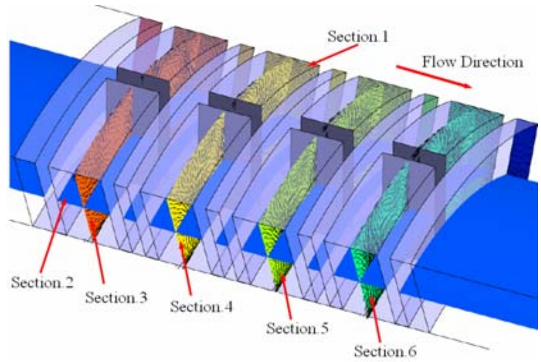

Fig. 14 The positions for the sections of the PDS

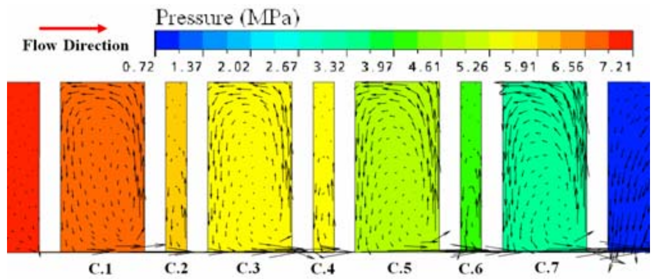

(a) PDS($S1 = 0.13mm$, $\pi = 0.13$, $n1 = 10200rpm$)

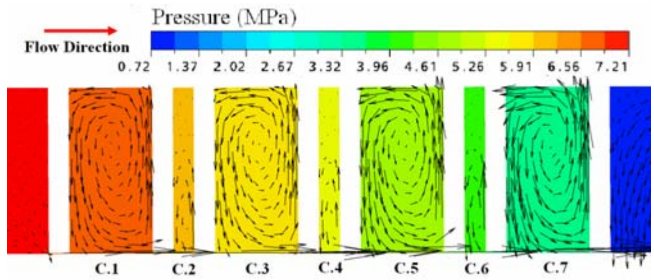

(b) Labyrinth seal($S1 = 0.13mm$, $\pi = 0.13$, $n1 = 10200rpm$)

Fig. 15 Static pressure contours and velocity distribution

The static pressure contours and velocity distribution of the meridional surface in the PDS and labyrinth seal are compared in Fig. 15. The meridional surface of the PDS is placed at the position of the Section 1 in Fig. 14. The pressure in two seals decrease along the chamber step by step and the flow patterns of two seal configurations are almost similar according to Fig. 15. The fluid passes the blade tip gap and separates two jets. One jet impinges on the subsequent blade and is deflected by

90°, then directed towards the top of the chamber and occurs a large recirculation zone. The other one directly enters the subsequent blade tip gap by kinetic energy carryover. The intensity of recirculation inside the active cavities (C.1, C.3, C.5, C.7) is stronger than that of the inactive cavities (C.2, C.4, C.6), especially for the downstream cavities. This means that inside the active cavities, larger viscous shear stress is generated to dissipate the jet kinetic energy efficiently.

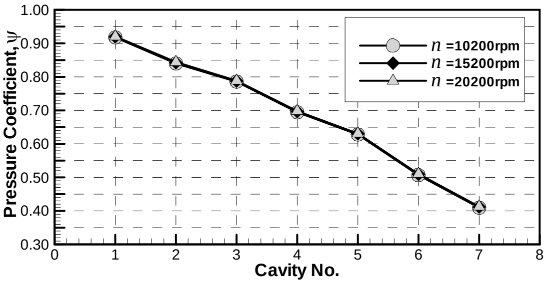

(a) PDS

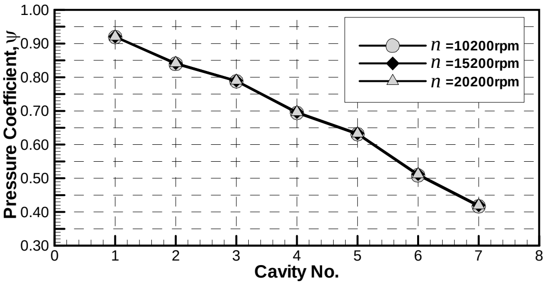

(b) Labyrinth seal

Fig. 16 Pressure coefficient in cavities of the PDS and the labyrinth seal at different rotational speeds($S1 = 0.13mm$, $\pi = 0.13$)

The dissipation mechanism is supported by the variation of mean cavity pressure in terms of the dimensionless pressure coefficient along the flow direction from seal inlet to exit as shown in Fig. 16. The same regressive behavior of the cavity pressure coefficients along the flow direction is observed at different rotational speeds for two seal configurations. The pressure coefficient drops through the downstream blade tip gaps of active cavities are clearly larger than those of inactive cavities, especially for the downstream cavities. According to equation (4), the pressure drop through the last blade accounts for 40% of the pressure drop across the over seal.

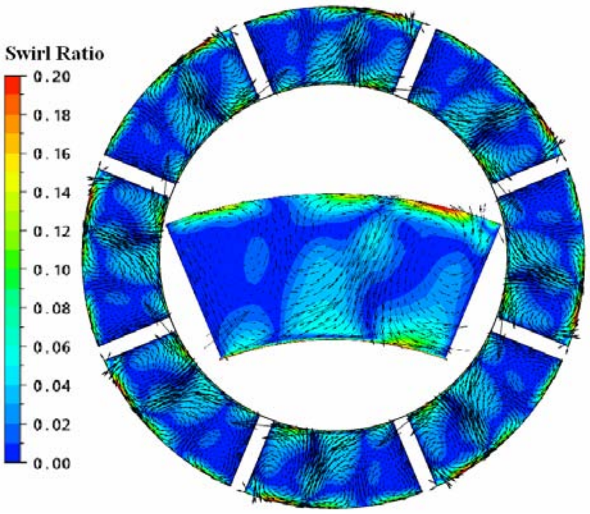

(a) section 1

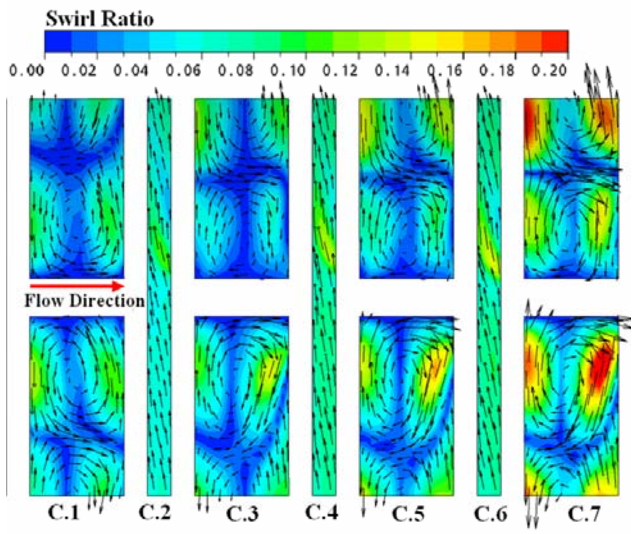

(b) section 2

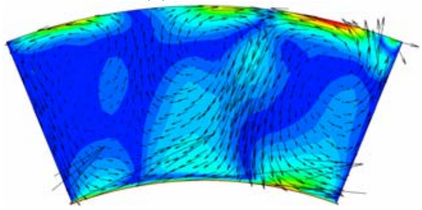

(c) section 3

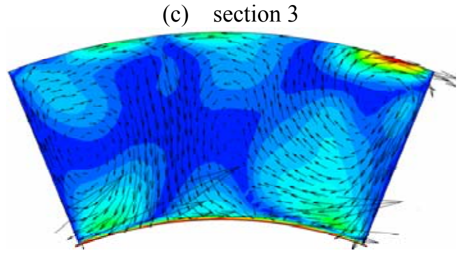

(d) section 4

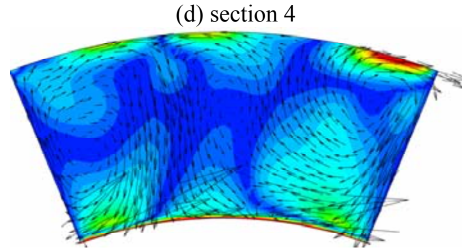

(e) section 5

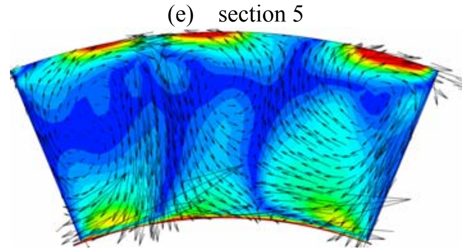

(e) section 6

Fig. 17 Swirl ratio contours and velocity distribution in the section of the active cavity of the PDS ($s1 = 0.13mm$, $\pi = 0.26$, $n1 = 10200rpm$)

The major difference between the PDS and the conventional labyrinth seal is that the PDS is designed with circumferential partition walls separating the active cavities of the seal into pockets. Therefore, the flow field in the section of the active cavity is the key to understand the flow mechanisms of the PDS. Fig. 17 gives the swirl ratio contours and velocity distribution in the axial sections of the active cavities in the

PDS. Due to the partition wall, the circumferential fluid driven by the viscous shear stress generated from the rotating shaft surface deflects at the solid wall and is limited inside the cavity. Inside the cavity, several three-dimensional different size recirculation zones occur, through which the circumferential velocity is reduced. Therefore, the flow field in the active cavity is quite complex. The intensity and the shape of the recirculation zones in the active cavity of the PDS change along the flow direction. The swirl ratio increases along the flow direction from seal inlet to exit due to the rotating shaft.

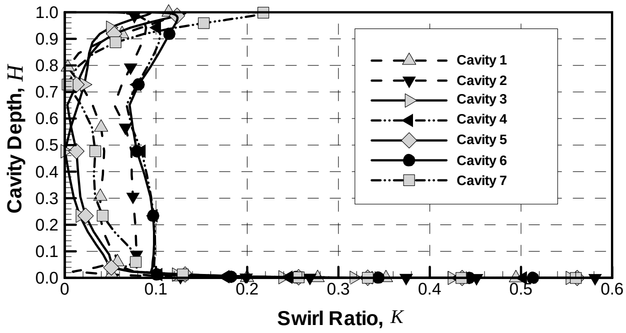

(a) $n1 = 10200rpm$

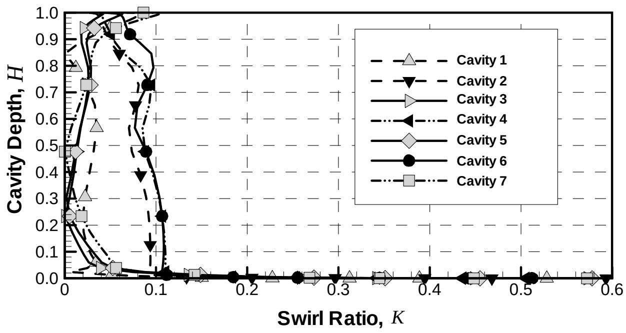

(b) $n2 = 15200rpm$

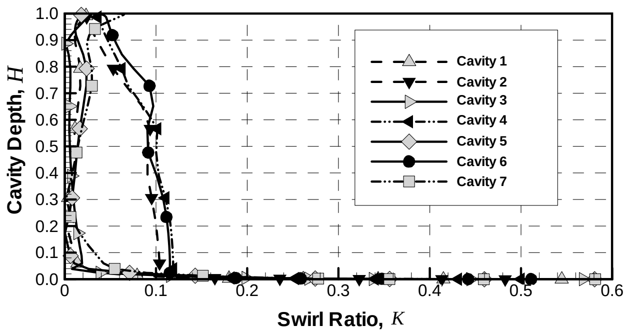

(c) $n3 = 20200rpm$

Fig. 18 Swirl ratio in the chambers of the PDS at different rotational speeds

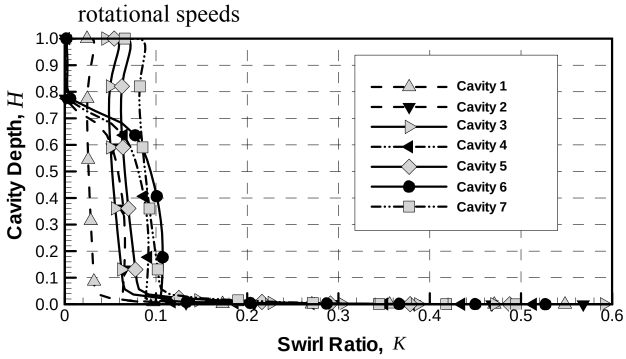

(a) $n1 = 10200rpm$

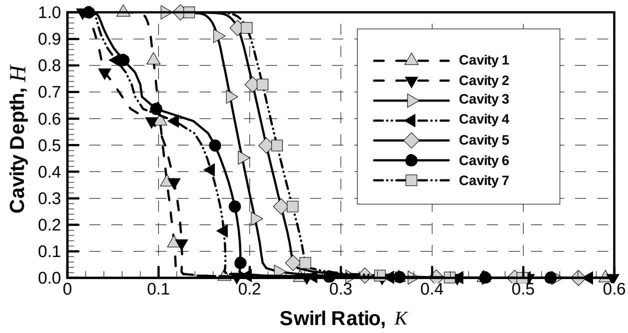

(b) $n2 = 15200rpm$

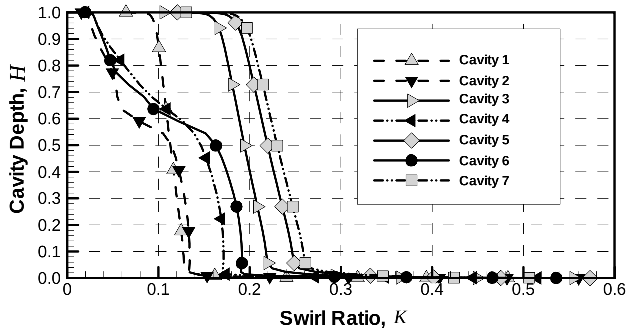

(c) $n3 = 20200rpm$

Fig. 19 Swirl ratio in the chambers of the labyrinth seal at different rotational speeds

Fig. 18 and Fig. 19 show the swirl development from seal inlet to exit of the PDS and the labyrinth seal, respectively. In Fig. 18 and Fig. 19, the radial position is plotted as the dimensionless cavity depth on the ordinate. The circumferential velocity is plotted as the dimensionless swirl ratio on the abscissa. As to the PDS, the swirl ratio in active cavity(C.1, C.3, C.5, C.7) is smaller than that of the inactive cavity(C.2, C.4, C.6). In addition, the difference of the swirl ratio between the active cavity and inactive cavity increases with increasing rotational speed. As to the labyrinth seal, the difference of the swirl ratio between the active cavity and inactive cavity is insignificant at lower rotational speed 10200rpm. The swirl ratio in the active cavity is larger than that of the inactive cavity at higher rotational speed. It can be seen that the swirl ratio in labyrinth seal depends more strongly on the rotational speed and has a significant increase along the flow direction. This can be explained by that the reduction of the circumferential flow in the active cavity of the PDS due to the partition wall. At the highest rotor speed 20200rpm, the swirl ratio in the active and inactive cavity of the PDS is reduced by 94.5% and 46% compared to the labyrinth seal, respectively. This indicates that the partition walls greatly reduce circumferential flow in the PDS, which is a desirable attributes from a rotordynamic stability point of view.

CONCLUSIONS

Based on experimental data, three-dimensional RANS solution was utilized to analyze the influence of pressure ratio, rotational speed, and sealing clearance on leakage characteristics of the PDS. Numerical investigations of the leakage characteristics were also carried out in the conventional labyrinth seal for comparison with the PDS.

As for the effect of the pressure ratio, the flow coefficient of the PDS increases with the decreasing pressure ratio and the trend is slowed down gradually. The flow coefficient asymptotically approaches a maximum value with pressure ratio decreasing. When pressure ratio is less than 0.22, the flow coefficient of the PDS becomes independent of the pressure ratio and the leakage flow across the last blade is choked.

As for the effect of the rotational speed, the flow coefficient of the PDS decreases with increasing circumferential Mach number at the fixed pressure ratio and sealing clearance, and this trend is more significant at higher circumferential Mach number. At circumferential Mach number 0.35(n=20200rpm), the flow coefficient is up to 4.4% less than that of the non-rotating case. Shaft growth due to the rotational speed is not taken into consideration for the effect of the rotational speed.

As for the effect of the sealing clearance, the increase in the flow coefficient of the PDS is approximate linearly proportional to the relative sealing clearance with slope 20.5 at the fixed pressure ratio and rotational speed.

The shaft growth due to the high rotational speed significantly influenced the leakage rate of the PDS, reducing the leakage rate by up to 6.35% at the highest rotational speed 20200rpm. This does go some way in explaining the phenomenon that the numerical approach used in present paper over predicts the leakage rate by a larger amount as the rotational speed increases.

The comparison of the leakage flow rate shows that the PDS leaks slightly less than the labyrinth seal at the same pressure ratio, rotational speed and sealing clearance, especially for the higher rotational speed. At the highest rotational speed 20200rpm, the leakage flow rate of the PDS is less than that that of the labyrinth seal by up to 1.9%.

The comparison of the flow field shows that the flow in the PDS is more complex than that of the labyrinth seal due to the circumferential partition walls. The partition walls greatly reduce circumferential flow in the PDS, which is a desirable attributes from a rotordynamic point of view. At the highest rotor speed 20200rpm, the swirl ratio in the active and inactive cavity of the PDS is reduced by 94.5% and 46% compared to the labyrinth seal, respectively.

ACKNOWLEDGEMENTS

The authors are grateful for the project 50976083 supported by National Natural Science Foundation and the Grants from Specialized Research Fund for the Doctoral Program of Higher Education (20100201110013) of China.

REFERENCES

[1] Lakshminarayana, B., 1996, Fluid Dynamics and Heat Transfer of Turbomachinery,Wiley, New York, pp.339-347.

[2] Thomas, H., 1958, ‘‘Instabile Eigenschwingungen von Turbinenla¨ufern angefacht durch die Spaltstro¨mungen Stopfbuschen und Beschauflungen,’’ Bull deL’AIM, 71, pp. 1039-1063.

[3] Lattime SB, and Steinetz BM., 2004, “Turbine Engine Clearance Control Systems: Current Practices and Future Directions,” J. Journal of Propulsion and Power, 120(2): pp. 302-311.

[4] Chupp, R. E., Ghasripoor, F., Turnquist, N. A., Demiroglu, M., and Aksit, M. F., 2002, “Advanced Seals for Industrial Turbine Applications: Dynamic Seal Development,” J. Propul. Power, 18(6), pp. 1260-1266.

[5] Chupp, R. E., Hendricks, R. C., Lattime, S. B., and Steinetz, B. M., 2006, “Sealing in Turbomachinery,” J. Propul. Power, 22(2), pp. 313-349.

[6] Ahmed J, Gamal M, John M., 2008, “Labyrinth Seal Leakage Tests: Tooth Profile, Tooth Thickness, and Eccentricity Effects,” J. ASME J. Eng. Gas Turibines Power, 130: 012510.

[7] Childs, D., and Vance, J., 1994, ‘‘Annular Seals as Tools to Control Rotordynamic Response of Future Gas Turbine Engines,’’ AIAA Paper 94-2804.

[8] Childs, D. W., and Wade, J., 2004, “Rotordynamic-Coefficient and Leakage Characteristics for Hole-Pattern-Stator Annular Gas Seals-Measurements Versus Predictions,” ASME J. Tribol., 126(2), pp. 326-333.

[9] Vance, J. and Schultz, R., 1993, ‘‘A New Damper Seal for Turbomachinery,’’Vibration of Rotating Systems, ASME DE, 60, September 1993.

[10] Li, J., and Vance, J. M., 1995, “Effects of Clearance and Clearance Ratio on Two and Three Bladed TAMSEALS, TRC-Seal-4-95,” Turbomachinery Laboratory Research Progress Report, Texas A&M University, College Station.

[11] Ransom, D., Li, J., San Andrés, L., and Vance, J. M., 1998, “Experimental Force Coefficients for a Two-Bladed Labyrinth Seal and a Four Pocket Damper Seal,” ASME J. Tribol., 28, pp. 98-109.

[12] Laos, H. E., 1999, “Rotordynamic Effect of Pocket Damper Seals,” Ph.D. dissertation, Texas A&M University.

[13] Li, J., Aguilar, R., San Andrés, L., and Vance, J. M., 2000, “Dynamic Force Coefficients of a Multiple Blade, Multiple-Pocket Gas Damper Seal: Test Results and Predictions,” ASME J. Tribol., Vol. 122, pp. 317-322.

[14] Laos, H. E., Vance, J. M., Buchanan, S. E., 2000, “Hybrid Brush Pockent Damper Seals for Turbomachinery,” ASME J. Eng. Gas Turibines Power, 122, pp. 330-336.

[15] Gamal, A. M., Ertas, B. H., and Vance, J. M., 2007, “High-Pressure Pocket Damper Seals: Leakage Rates and Cavity Pressures,” ASME J. Turbo., Vol. 129, pp. 826-834.

[16] Childs, D. W. and Vance, J. M., 1997, “Annular Gas Seals and Rotordynamics of Compressors and Turbines,” Proceedings of 26th Turbomachinery Symposium, Texas A&M University, College Station, TX, pp. 201-220.

[17] Ertas, B., 2005, “Rotordynamic Force Coefficients of Pocket Damper Seals,”Ph.D. Dissertation in Mechanical Engineering, May 2005, Texas A&M University.

[18] Vance, J. M., and Li, J., 1996, “Test Results of A New Damper Seal for Vibration Reduction in Turbomachinery,” ASME J. Eng. Gas Turibines Power, Vol. 118, pp. 843-846.

[19] Li, J., San Andre´s, L., and Vance, J. M., 1999, “A Bulk-Flow Analysis of Multiple-Pocket Gas Damper Seals,” ASME J. Eng. Gas Turibines Power, Vol. 121, No. 2, pp. 355-362.

[20] Li, J., Ransom, D., San Andre´s, L., and Vance, J. M., 1999, “Comparison of Predictions with Test Results for Rotordynamic Coefficients of a Four-Pocket Gas Damper Seal,”, ASME J. Tribol., Vol. 121, 2, pp. 363-369.

[21] Li, J., Aguilar, R., San Andrés, L., and Vance, J. M., 2000, “Dynamic Force Coefficients of a Multiple Blade, Multiple-Pocket Gas Damper Seal: Test Results and Predictions,” ASME J. Tribol., 122, pp. 317-322.

[22] Li, J., Kushner, F., and DeChoudhury, P., 2002, “Experimental Evaluation of Slotted Pocket Damper Seals on a Rotating Test Rig,” The 47th ASME TurboExpo Land Sea &Air, pp. 230-240.

[23] AEA Technology GmbH, 2004, CFX-TASCflow User Documentation, AEA Technology, Software Ltd., Canada.

[24] Denecke, J., Farber, J., Dullenkopf, K., and Bauer, H. J., 2008, “Interdependence of Discharge Behavior, Swirl Development and Total Temperature Increase in Rotating Labyrinth Seals”, ASME Paper: GT2008-51429.

